STATISTICS, OPTIMIZATION AND INFORMATION COMPUTING
Stat., Optim. Inf. Comput., Vol. **x**, Month 2024, pp 0–8.
Published online in International Academic Press (www.IAPress.org)

Speed Control of a PMSM drive system using a nonsingular terminal sliding mode controller

Yahia Mazzi [1,*], Hicham Ben Sassi [1,2], Fatima Errahimi [1], Najia Es-Sbai [1]

[1] *Laboratory of Intelligent Systems, Georesources and Renewable Energies (LISGRE), Faculty of Sciences and Technology, Sidi Mohamed Ben Abdellah University. Fez, Box 2202, Fez, Morocco*
[2] *Department of electrical engineering, Royal School of Aeronautics, Marrakech, Morocco*

Abstract Due to its dependability, high accuracy, and performance, the permanent magnet synchronous motor (PMSM) is becoming an attractive option for electric vehicle traction systems. In this context, the objective is to achieve high power conversion efficiency and high mechanical speeds with great precision. Therefore, motor control is of paramount importance in EVs as a vehicle on the road is prone to various disturbances and load variations. Hence, a robust speed controller is necessary to ensure high operational performance, precise speed tracking, minimal overshoot, and disturbance rejection. In this study, a nonsingular terminal sliding mode controller (NTSMC) is proposed for the speed control of a PMSM powered by a three-phase voltage source inverter (VSI). NTSMC is a well-established method that provides high-performance control and can effectively handle parameter uncertainties and disturbances, making it highly suitable for PMSM speed control. The stability of the NTSMC is validated using Lyapunov stability theory. Finally, several simulations are performed. The proposed method demonstrates through simulations that it surpasses the conventional proportional-integral (PI) controller. Additionally, it provides precise speed tracking, high-performance control, and reduced overshoot, proving its feasibility and effectiveness.

Keywords Permanent magnet synchronous motor, nonsingular terminal sliding mode controller, nonlinear control, field-oriented control, speed controller

DOI: 10.19139/soic-2310-5070-1913

1. Introduction

A significant contributor to climate change and global warming is the greenhouse gas (GHG) emissions from fossil fuels [1]. Recent statistics estimate that the transportation sector accounts for 14% of global GHG emissions [2]. To address this issue, many countries and governments are revamping their transportation sectors to reduce GHG emissions [3]. One of the most effective strategies is to adopt electromobility by replacing traditional vehicles with electric vehicles (EVs) or hybrid electric vehicles (HEVs) that use electric motors instead of internal combustion engines (ICE). The propulsion system, which is the core component of an EV, consists of three parts: an energy storage system (ESS), power electronic converters, and an electric motor. The ESS supplies the necessary power to drive the vehicle and power other onboard devices. It typically comprises thousands of Lithium-ion cells that are carefully managed to ensure a safe and reliable rechargeable battery [4, 5]. Power electronic converters, on the other hand, serve as the power transfer bridge between components with different electrical characteristics. Specifically, various DC-DC converters can step up or step down a DC voltage from one side to another [6]. Meanwhile, the DC-AC converter, or inverter, can convert a DC voltage to an AC voltage to power loads operating with three-phase or single-phase power. In EVs, this type of converter is mainly used to supply the electric motor, which converts

*Correspondence to: Yahia Mazzi (Email: yahia.mazzi@usmba.ac.ma). Laboratory of Intelligent Systems, Georesources and Renewable Energies (LISGRE), Faculty of Sciences and Technology, Sidi Mohamed Ben Abdellah University. Fez, Box 2202, Fez, Morocco.

ISSN 2310-5070 (online) ISSN 2311-004X (print)

electrical energy into the mechanical energy needed to drive the vehicle. This paper specifically focuses on the electric motor of the EV.

For high-performance electric vehicles (EVs), the electric motor needs to meet several essential criteria such as a simple structure, compact size, low noise, high efficiency, ease of control, a broad speed range, durability, and high power density. To achieve these goals, various electric motors with different designs and technological innovations have been suggested in the literature for EVs. These include induction motors (IM), synchronous reluctance motors (SynRM), permanent magnet synchronous motors (PMSM), and switched reluctance motors (SRM). Among these motor technologies, the PMSM is typically the most suitable for automotive requirements [7]. Additionally, the PMSM is primarily distinguished by its simple structure, high efficiency, high power density, and wide speed range [8].

Given that the PMSM exhibits significant nonlinearity and is prone to external disturbances and parameter fluctuations in real-world driving scenarios, it is essential to have a dependable and robust speed controller to ensure stable vehicle operation and passenger comfort. Consequently, to attain high precision and robust control of PMSM speed, various controllers have been documented in the literature.

In recent times, the field-oriented control (FOC) scheme has been widely adopted because of its straightforward structure, ease of implementation, rapid dynamic response, and minimal torque ripple. Furthermore, FOC based on PI controllers simplifies modeling by decoupling the controller into two control loops [9]. The first is the external control loop, where a speed controller is introduced to ensure precise tracking. Conversely, the second is the internal control loop, where the d-q frame currents are independently controlled to regulate the d-q currents and generate reference voltages. However, this control scheme often fails to achieve the desired performance and precision, reduces dependency on the model's parameters, and mitigates the impact of disturbances [10]. A state feedback controller for PMSM, which employs Jacobian linearization and a disturbance observer for load torque, is proposed in [11]. Additionally, due to their ability to provide efficient tracking performance even in the presence of disturbances, sliding mode controllers (SMC) are commonly used to control nonlinear systems. Accordingly, a conventional SMC and a tangent function-based phase-locked loop (PLL) technique are adopted in [12] for sensorless control of PMSM. However, the chattering effect associated with conventional SMC remains an issue. The integral SMC (ISMC) can slightly mitigate this effect by incorporating an integral term in the sliding manifold [13]. Moreover, other advanced algorithms based on SMC are explored to reduce chattering and enhance the controller's dynamic response. For example, terminal SMC (TSMC) and fast terminal SMC (FTSMC) can both force the tracking error to converge to zero in finite time [14]. Nonetheless, the use of fractional power in the sliding surface variable of these methods leads to the singularity problem. Therefore, to address this issue, the Nonsingular terminal SMC is highly recommended [15].

Considering the vehicle's vulnerability to various disturbances impacting the motor and controller performance, this paper explores a robust approach utilizing NTSMC for PMSM speed. Furthermore, this method effectively rejects lumped disturbances and minimizes the chattering phenomenon. To simplify control complexity and ease implementation constraints, two PI controllers are incorporated into the current control loops.

The remainder of this paper is structured as follows. Section 2 outlines the system model. Section 3 describes the proposed control strategy. Section 4 presents the simulation results and discusses their interpretation. Lastly, in Section 5, the conclusions derived from this study are presented.

2. Mathematical model of the PMSM

In order to simplify the modeling and control strategy without degrading the precision of the system, in this document the following assumptions are adopted regarding PMSM are adopted.

- *Neglecting the Damper Winding Effect:* The focus in this paper remains on the steady-state and dynamic performance of the control strategy without the added complexity of transient damping effects. Thus, the damper windings, typically present in some machines to provide damping torque, are ignored.

- *Ignoring Iron Losses:* The iron losses, which include hysteresis and eddy current losses in the stator and rotor core, are not considered in this model. This assumption is made to streamline the analysis, focusing on the dominant electrical and mechanical dynamics.
- *Sinusoidal Magnetic Field Distribution:* It is assumed that the magnetic field distribution in the air gap is sinusoidal. This is a standard assumption for surface-mounted PMSMs, which simplifies the model by allowing the use of sinusoidal back EMF equations.

Under these assumptions, the mathematical model of the PMSM in the synchronous rotating d-q frame is described by the following equations:

$$\frac{di_d}{dt} = -\frac{R_s}{L_d} i_d + N_p \omega_m i_q + \frac{1}{L_d} V_d \tag{1}$$

$$\frac{di_q}{dt} = -\frac{R_s}{L_q} i_q - N_p \omega_m i_d - \frac{N_p \lambda_m}{L_q} + \frac{1}{L_q} V_q \tag{2}$$

$$\frac{d\omega_m}{dt} = \frac{T_e}{J} - \frac{B}{J}\omega_m - \frac{T_L}{J} \tag{3}$$

$$T_e = \frac{3}{2} N_p \left(\lambda_m i_q + (L_d - L_q) i_d i_q\right) \tag{4}$$

Where i_d, V_d, and L_d are respectively the current, voltage, and stator inductance in the d-axis, while i_q, V_q, and L_q are their respective values in the q-axis. B is the viscous coefficient, J is the moment of inertia, T_L is the load torque, T_e is the electromagnetic torque, R_s is the stator resistance, N_p is the pole pairs count, λ_m is the permanent magnet flux linkage, ω_m is the mechanical angular speed, and f represents the lumped disturbances.

In the above model, Eq. 1 and Eq. 2 represent the dynamics of the d-q-axis currents, taking into account stator resistance, inductance, and the interaction between the d-q-axis components due to rotor angular velocity. Eq. 3 details the mechanical dynamics of the rotor by considering also external disturbances. While Eq. 4 provides the general expression for the electromagnetic torque, taking into account the interaction of the d-q axis currents and inductances. In this paper, the motor is assumed to be a surface-mounted PMSM (SM-PMSM), where the d-q axis inductances are set as $L_d = L_q = L_s$. Therefore, the electromagnetic torque becomes:

$$T_e = \frac{3}{2} N_p \lambda_m i_q \tag{5}$$

On the basis of the above dynamic equations of the PMSM, it is clear that the system is nonlinear and susceptible to lumped disturbances. Therefore, a robust and accurate speed controller is demanded to guarantee high-tracking performance and disturbance rejection

3. PMSM speed controller design

Generally, the main objectives set for any speed controller are; to regulate the PMSM speed so that it matches the desired value ω_m^* provided by the EV's driver and to react quickly and accurately to any speed changes or disturbances. Therefore, in this work, a robust NTSMC is introduced to achieve these objectives. Similarly like conventional SMC, this method is a nonlinear approach that operates by dragging the system states towards a predetermined hyperplane called the "sliding surface". Then a discontinuous control signal is used to keep the system confined to the sliding surface. The general structure of the proposed strategy is illustrated in Fig. 1, in which the control strategy is divided into two subsystems, the external control loop and the internal control loop.

In the FOC scheme, the internal control loop requires two input references: the d-axis current i_d^* and q-axis current i_q^*. For maximum torque per ampere (MTPA), the i_d^* reference is set to zero. The reference i_q^* is determined by the external control loop, which uses the proposed NTSMC. These references, i_d^* and i_q^*, are then fed into the internal control loop. In this paper, a PID controller within the internal control loop generates the reference voltages V_d^* and V_q^* that correspond to the desired reference currents. These reference voltages are transformed

into the stationary $(\alpha,\ \beta)$ frame using Clark's transform. Finally, space vector pulse width modulation (SVPWM) is employed to generate the appropriate three-phase voltages supplied to the motor.

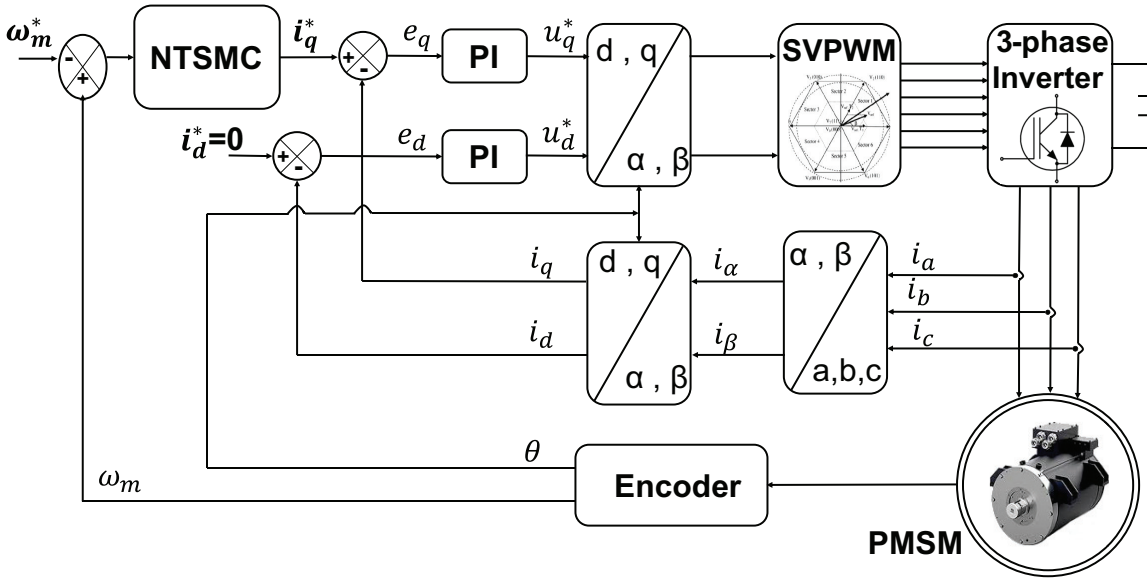

Figure 1. Schematic diagram of the proposed controller for PMSM.

3.1. External control loop

Since the controller's objective is to track the reference speed ω_m^* of the PMSM, the tracking error is defined as $e_\omega = (\omega_m - \omega_m^*)$. Taking into account the disturbances, the second-order auxiliary system can be designed by defining the auxiliary variables as follows $x_1 = e_\omega$ and $x_2 = \dot{e}_\omega$:

$$\begin{cases} x_1 & = \omega_m - \omega_m^*, \\ x_2 & = \dot{\omega}_m = \frac{3}{2}\frac{N_p\lambda_m}{J} i_q - \frac{B}{J}\omega_m + f(t) \end{cases} \tag{6}$$

Unlike the conventional SMC, the NTSMC uses a nonlinear sliding surface defined in Eq. 7. This surface is designed to improve the convergence properties of the controller. Specifically, the $x_2^{\frac{l}{m}}$ term ensures faster, finite-time convergence to the sliding surface, and avoids the singularity issue compared with the linear sliding surfaces used in conventional SMC. This design choice enhances the robustness and accuracy of the control system, particularly for handling parameter uncertainties and external disturbances.

$$s_\omega = x_1 + \frac{1}{\gamma} x_2^{\frac{n}{m}} \tag{7}$$

where γ is a positive constant gain, and both n and m are positive odd integers satisfying the condition: $1 < \frac{n}{m} < 2$.

Assuming that the disturbances are bounded to satisfy $|f(t)| < \delta$ and $\left|\dot{f}(t)\right| < \varepsilon$, where δ and ε are positive constants, the global control law of the system defined in Eq. 6 is designed as follows:

$$i_q^* = i_q^{eq} + i_q^{st} \tag{8}$$

$$i_q^* = \frac{2J}{3N_p\lambda_m}\left(\frac{B}{J}x_1 - \gamma\frac{m}{n}\int_0^t x_2^{2-\frac{n}{m}}d\tau - K_s\,\mathrm{sign}(s_\omega)\right) \tag{9}$$

where $i_q^{st} = -K_s \operatorname{sign}(s_\omega)$ is the switching control law, i_q^{eq} is the equivalent control law, $\operatorname{sign}(s_\omega)$ denotes the discontinuous sign function, and $K_s = (\varepsilon + k)$ is a positive switching gain.

Afterward, the stability of the speed controller is verified using the Lyapunov stability theory. In this regard, the Lyapunov function is chosen as $V = \frac{1}{2}s_\omega^2$, and its first-time derivative is given as:

$$\dot{V} = s_\omega \dot{s}_\omega = s_\omega \left(x_2 + \frac{n}{m\gamma} \dot{x}_2 x_2^{\frac{n}{m}-1} \right) \tag{10}$$

Subsequently, Eq. 11 is obtained by substituting $\dot{x}_2$ and i_q^* by their expressions in Eq. 10:

$$\dot{V} = s_\omega \frac{n}{m\gamma} x_2^{\frac{n}{m}-1} \left(\dot{f}(t) - K_s \operatorname{sgn}(s_\omega) \right) \tag{11}$$

$$\dot{V} < -K_s \frac{n}{m\gamma} s_\omega x_2^{\frac{n}{m}-1} \tag{12}$$

For $x_2 \neq 0$ and $1 < \frac{n}{m} < 2$, $K_s \frac{n}{m\gamma} x_2^{\frac{n}{m}-1}$ is positive. Hence, $\dot{V} < -\mu s_\omega$, which satisfies the stability condition of Lyapunov. In the case where $x_2 = 0$, the stability is also maintained, as explained in [**?**]. K_s is chosen high enough to eliminate the lumped disturbances. Finally, by adopting the NTSMC approach, the hyperplane surface (Eq. 7) can be achieved in finite time; hence, the tracking error will reach the equilibrium state in the same fashion.

3.2. Internal control loop

According to Eq. 5, i_q is the sole current responsible for generating torque. Consequently, the direct current i_d is set to zero to optimize performance and achieve MTPA. To balance the complexity and performance of the controller, the current control loop employs two PI controllers to manage the d-q currents individually. While it is possible to use a more advanced controller to enhance tracking performance, this paper opts for the conventional PI controller due to the complexity and implementation challenges of advanced controllers. As shown in Fig. 1, the d-q reference voltages generated by the two current loops are utilized by the SVPWM to create the appropriate switching states for the inverter gates. Subsequently, the DC-bus voltage is used to produce an alternating current (AC) wave to drive the SM-PMSM at various speeds.

4. Results and discussions

To illustrate the dependability and robustness of the proposed controller, two case studies are presented in this section. Additionally, the available PMSM parameters from a Nissan Leaf S are utilized for more realistic simulation. Table 1 outlines the main parameters of the employed SM-PMSM. The PI controller parameters of the internal control loop are adjusted to ensure that the $d-q$ currents respond quickly. Therefore, the following values are used to meet this requirement: $K_{q,p} = 10$, $K_{q,i} = 90$, $K_{d,p} = 10$, and $K_{d,i} = 90$. The NTSMC parameters are also fine-tuned repeatedly to achieve finite-time convergence and precise tracking. Consequently, the parameter values are: $n = 10$, $m = 10$, $\gamma = 10$, and $K_s = 10$. The inverter gate switching frequency is set to $f_s = 10$ kHz.

Case 1: In this scenario, the simulation is conducted for a total duration of 2 seconds with a high reference speed set at 1000 rpm. A load torque of 20 N.m is applied at the 1-second mark and is removed at 1.6 seconds. The speed response is depicted in Fig. 2, while the tracking error is shown in Fig. 3. Unlike the NTSMC, the PI controller exhibits a significant overshoot of approximately 336 rpm. Additionally, the settling time for the proposed controller (0.116 seconds) is significantly shorter than that of the PI controller (0.280 seconds), demonstrating the superiority of the NTSMC. This is further corroborated by the speed drops observed at t = 1 second. Specifically, the NTSMC results in a speed drop of only 4 rpm lasting less than 0.005 seconds, compared to a 72 rpm drop by the PI controller lasting 0.08 seconds. Moreover, it is evident that the PI controller's response shows high ripples during transition phases, which is not observed with the NTSMC. The steady-state accuracy of the NTSMC is higher than that of the PI controller, as illustrated in Fig. 2. Thus, the proposed controller demonstrates precise and robust speed tracking with a rapid dynamic response.

Table 1. The basic parameters of PMSM

Parameter	**Value**	**Parameter**	**Value**
Rated power, P_m	110 KW	Rated voltage, V_r	360 V
Rated speed, rpm	3283 rpm	Maximum torque, $T_{\max}$	320 N.m
Pole pairs, N	8	Moment of inertia, J	0.0280 $Kg.m^2$
Flux linkage, λ_m	0.133 Wb	Viscous coefficient, B	0.00034 N.m.s
Stator inductance, L_s	0.89858 mH	Stator resistor, R_s	0.0201 Ω

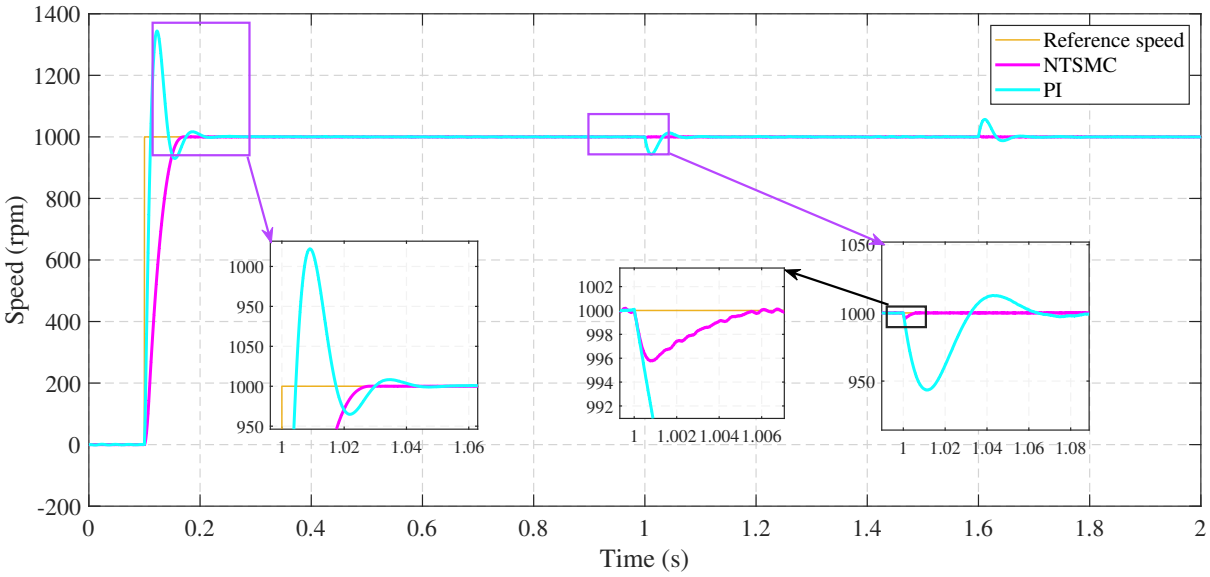

Figure 2. Speed response of PMSM under different controllers of case 1.

Case 2: In this case, a more demanding driving profile is performed, where the PMSM experiences varying speeds, load torque fluctuations (Fig. 4(a)), and flux linkage uncertainties (Fig. 4(b)). Fig. 5 displays the speed response waveforms. From the results shown in Fig. 5, it is clear that rapid and sudden load torque changes have a minimal impact on the NTSMC tracking performance. Conversely, the PI controller exhibited a noticeable speed drop whenever the load torque varied. Additionally, to assess the controller's robustness to PMSM internal parameter uncertainties, this study employs a variable rotor flux linkage. It is observed that NTSMC remains robust to these uncertainties, with no effect on speed tracking accuracy due to flux linkage variations. This is not true for the PI controller, which showed significant speed drops, particularly when the flux linkage returned to its nominal value at t=3.3s, resulting in a speed drop of approximately 40 rpm.

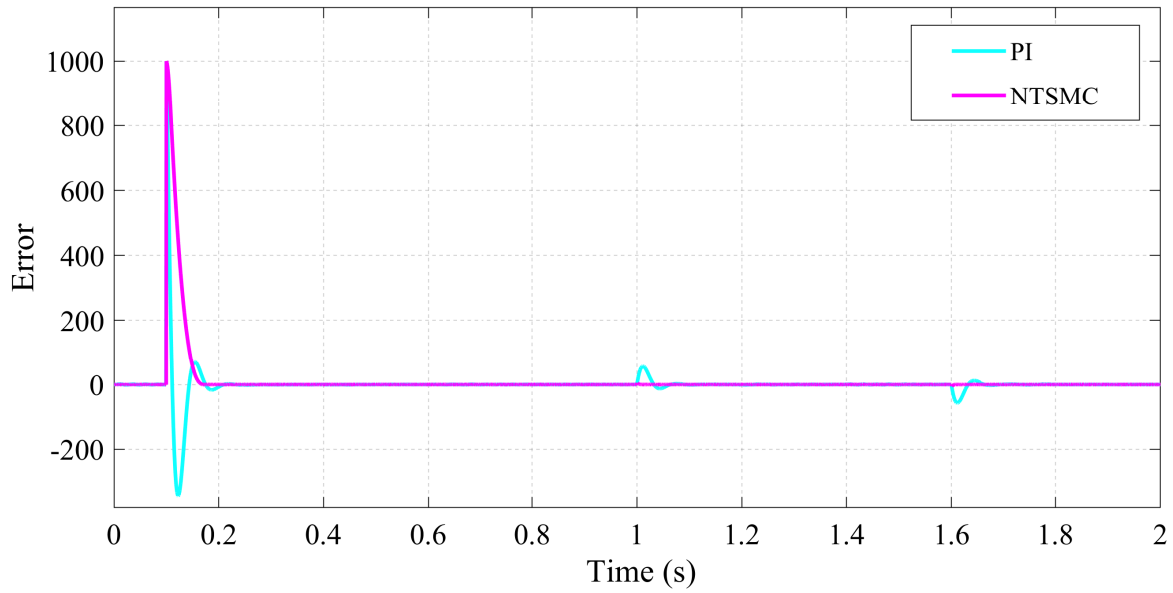

Figure 3. Tracking error under different controllers of case 1.

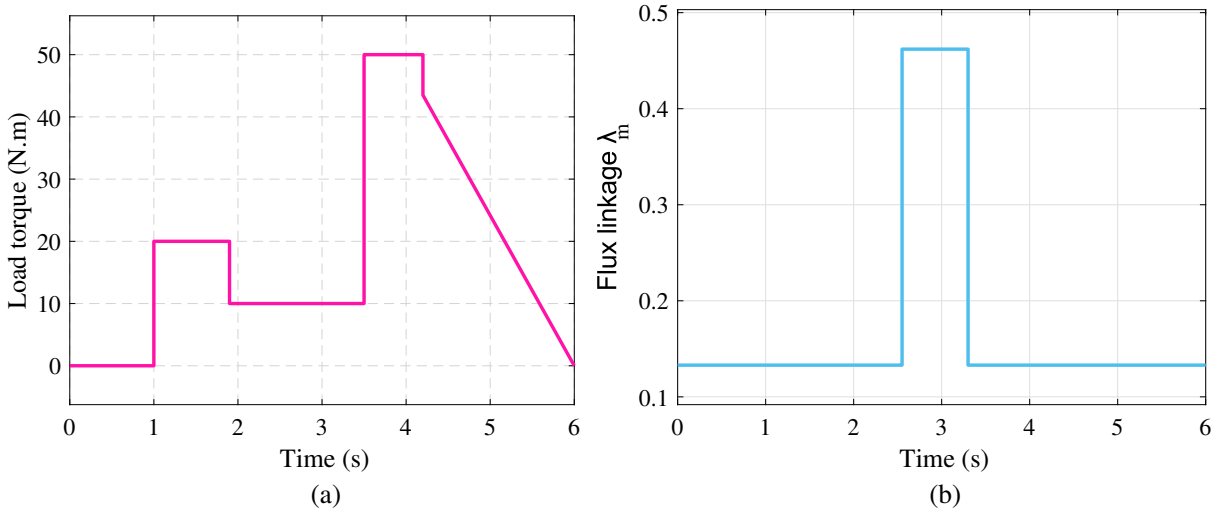

Figure 4. Load torque and flux linkage profiles used in case 2.

5. Conclusion

Due to its high efficiency, simple design, and high power density, the PMSM is extensively used in contemporary EVs. In these applications, high levels of accuracy and precision are crucial to ensure the vehicle operates reliably and safely under various driving conditions. Consequently, this paper introduces a nonlinear controller based on NTSMC to regulate the PMSM speed to a reference value set by the vehicle's driver. The controller's stability

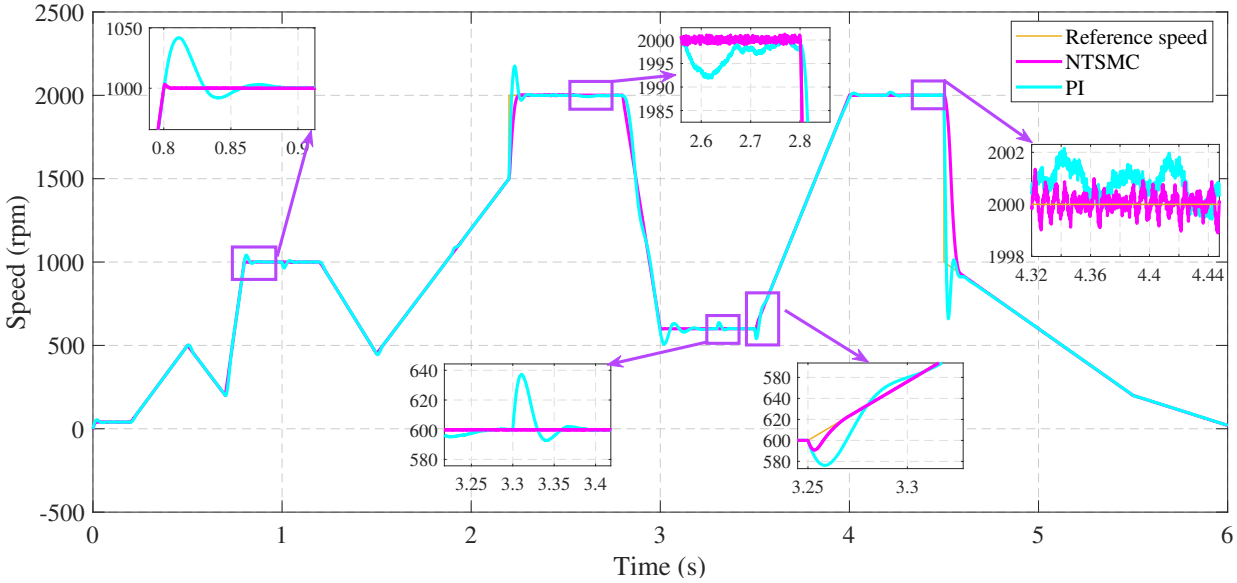

Figure 5. Speed response of PMSM under different controllers of case 2.

has been confirmed using the Lyapunov stability theory. To validate the proposed approach's performance and robustness, the system was tested under various driving conditions by altering the reference speed, applying different load torque values, and modifying the rotor's flux linkage to simulate uncertainties in the motor's internal parameters. The simulation results demonstrate that the NTSMC provides high tracking accuracy and excellent anti-disturbance performance. In this context, the system maintained stability despite load variations and parameter uncertainties. Therefore, the authors suggest implementing this controller in EV motor controllers. However, it is important to note that the increased computational complexity may present challenges for real-time implementation. To further evaluate the proposed controller's effectiveness, a hardware-in-the-loop (HIL) setup will be implemented in future work. Additionally, an estimator of the rotor angle will be used in the HIL to reduce the control system's cost.

REFERENCES

1. I. Gunnarsdóttir, B. Davidsdóttir, E. Worrell, and S. Sigurgeirsdóttir, *Sustainable energy development: History of the concept and emerging themes*, Renewable and Sustainable Energy Reviews, vol. 141, p. 110770, 2021.
2. K. Moustakas, M. Loizidou, M. Rehan, and A. S. Nizami, *A review of recent developments in renewable and sustainable energy systems: Key challenges and future perspective*, Renewable and Sustainable Energy Reviews, vol. 119, p. 109418, 2020.
3. H. Ben Sassi, C. Alaoui, F. Errahimi, and N. Es-Sbai, *Vehicle-to-grid technology and its suitability for the Moroccan national grid*, Journal of Energy Storage, vol. 33, p. 102023, 2021.
4. Y. Mazzi, H. Ben Sassi, A. Gaga, and F. Errahimi, *State of charge estimation of an electric vehicle's battery using tiny neural network embedded on small microcontroller units*, International Journal of Energy Research, vol. 46, no. 6, pp. 8102–8119, 2022.
5. Y. Mazzi, H. Ben Sassi, F. Errahimi, and N. Es-Sbai, *State of charge estimation using extended Kalman filter*, in *2019 International Conference on Wireless Technologies, Embedded and Intelligent Systems (WITS)*, pp. 1–6, 2019.
6. M. Errouha, H. Hicham, and Z. CHALH, *Modelling and Simulation of the Hybrid System PV-Wind*, Statistics, Optimization & Information Computing, vol. 11, no. 1, pp. 143–153, 2023.
7. Y. Zheng, H. Zhao, S. Zhen, and H. Sun, *Fuzzy-set theory based optimal robust constraint-following control for permanent magnet synchronous motor with uncertainties*, Control Engineering Practice, vol. 115, p. 104911, 2021.
8. X. Zhao and S. Niu, *A new slot-PM vernier reluctance machine with enhanced zero-sequence current excitation for electric vehicle propulsion*, IEEE Transactions on Industrial Electronics, vol. 67, no. 5, pp. 3528–3539, 2019.
9. N. H. Hadi and I. K. Ibraheem, *Speed control of an SPMSM using a tracking differentiator-PID controller scheme with a genetic algorithm*, International Journal of Electrical and Computer Engineering, vol. 11, no. 2, p. 1728, 2021.

10. F. Mohd Zaihidee, S. Mekhilef, and M. Mubin, *Robust speed control of PMSM using sliding mode control (SMC)—A review*, Energies, vol. 12, no. 9, p. 1669, 2019.
11. A. Apte, V. A. Joshi, H. Mehta, and R. Walambe, *Disturbance-observer-based sensorless control of PMSM using integral state feedback controller*, IEEE Transactions on Power Electronics, vol. 35, no. 6, pp. 6082–6090, 2019.
12. S. Lin and W. Zhang, *An adaptive sliding-mode observer with a tangent function-based PLL structure for position sensorless PMSM drives*, International Journal of Electrical Power & Energy Systems, vol. 88, pp. 63–74, 2017.
13. Q. Song and C. Jia, *Robust speed controller design for permanent magnet synchronous motor drives based on sliding mode control*, Energy Procedia, vol. 88, pp. 867–873, 2016.
14. X. Yu, Y. Feng, and Z. Man, *Terminal sliding mode control–an overview*, IEEE Open Journal of the Industrial Electronics Society, vol. 2, pp. 36–52, 2020.
15. D. Cruz-Ortiz, I. Chairez, and A. Poznyak, *Non-singular terminal sliding-mode control for a manipulator robot using a barrier Lyapunov function*, ISA Transactions, vol. 121, pp. 268–283, 2022.